The EMBO Journal Vol. 20 No. 21 pp. 5971–5981, 2001

The pre-autophagosomal structure organized by concerted functions of *APG* genes is essential for autophagosome formation

Kuninori Suzuki[1,2], Takayoshi Kirisako[1,2], Yoshiaki Kamada[1,2], Noboru Mizushima[1,3], Takeshi Noda[1,2] and Yoshinori Ohsumi[1,2,4]

[1]Department of Cell Biology, National Institute for Basic Biology, Nishigonaka 38, Myodaiji-cho, Okazaki 444-8585, [2]Department of Molecular Biomechanics, School of Life Science, The Graduate University for Advanced Studies and [3]PRESTO, Japan Science and Technology Corporation, Japan

[4]Corresponding author
e-mail: yohsumi@nibb.ac.jp

Macroautophagy is a bulk degradation process induced by starvation in eukaryotic cells. In yeast, 15 Apg proteins coordinate the formation of autophagosomes. Several key reactions performed by these proteins have been described, but a comprehensive understanding of the overall network is still lacking. Based on Apg protein localization, we have identified a novel structure that functions in autophagosome formation. This pre-autophagosomal structure, containing at least five Apg proteins, i.e. Apg1p, Apg2p, Apg5p, Aut7p/Apg8p and Apg16p, is localized in the vicinity of the vacuole. Analysis of *apg* mutants revealed that the formation of both a phosphatidylethanolamine-conjugated Aut7p and an Apg12p–Apg5p conjugate is essential for the localization of Aut7p to the pre-autophagosomal structure. Vps30p/Apg6p and Apg14p, components of an autophagy-specific phosphatidylinositol 3-kinase complex, Apg9p and Apg16p are all required for the localization of Apg5p and Aut7p to the structure. The Apg1p protein kinase complex functions in the late stage of autophagosome formation. Here, we present the classification of Apg proteins into three groups that reflect each step of autophagosome formation.

Keywords: APG/autophagosome/autophagy/GFP/membrane dynamics

Introduction

During macroautophagy in yeast, a portion of the cytoplasm is non-selectively sequestered into double-membrane structures (autophagosomes) and delivered to the vacuole for degradation. Electron microscopic analysis revealed that autophagosomes fuse with the vacuolar membrane to release the inner membrane structure into the lumen (Baba *et al*., 1994). Autophagosomes are generated when a cup-shaped membrane sac (isolation membrane) extends to enwrap and seal cytoplasmic materials. This elongation process, accompanied by the assembly of membranous structures (Kirisako *et al*., 1999), is currently not well characterized. In mammalian cells, autophagosomes are generated in a similar manner. In rat hepatocytes, osmiophilic membranes designated as phagophores were observed under an electron microscope (Seglen, 1987; Fengsrud *et al*., 1995, 2000). In mouse embryonic stem cells, similar isolation membranes were identified by electron microscopy as precursors of autophagosomes (Mizushima *et al*., 2001). To understand the molecular mechanism controlling autophagy, we isolated 15 mutants defective in autophagy (*apg*) in yeast (Tsukada and Ohsumi, 1993) with disorders of bulk protein degradation, sporulation and the maintenance of viability under starvation conditions (Klionsky and Ohsumi, 1999). A vacuolar hydrolase aminopeptidase I (API) was constitutively transported to the vacuole via small double-membrane vesicles (Scott *et al*., 1997). This cytosol-to-vacuole targeting (Cvt) pathway runs under growing conditions. Extensive overlaps have been found in genes involved in the *APG*, *AUT* (autophagy) and *CVT* pathways (Harding *et al*., 1996). All *apg* mutants except *apg17* are known to be defective in the Cvt pathway.

Recent characterization of the Apg proteins has identified two ubiquitin-like systems utilizing approximately half of the Apg proteins. Apg12p, a ubiquitin-like protein, is covalently attached to Apg5p to form an Apg12p–Apg5p conjugate controlled by the serial action of Apg7p and Apg10p (Mizushima *et al*., 1998). Apg7p, a member of the E1-like activating enzymes, forms a thioester linkage with Apg12p (Kim *et al*., 1999; Tanida *et al*., 1999; Yuan *et al*., 1999). Apg12p subsequently forms a thioester intermediate with Apg10p, an E2 conjugating enzyme (Shintani *et al*., 1999). Apg12p is then linked to Lys149 of Apg5p through an isopeptide bond with the C-terminal glycine. Apg16p then interacts through its C-terminal coiled-coil region to form homo-oligomers following direct interaction with the Apg12p–Apg5p conjugate (Mizushima *et al*., 1999). In mammalian cells, a homologue of the Apg12p–Apg5p conjugate transiently associates with the membranes of precursor autophagosomes (Mizushima *et al*., 2001).

Aut7p/Apg8p, a second ubiquitin-like protein involved in autophagy, is conjugated to phosphatidylethanolamine (PE; Aut7p–PE) by the serial action of three Apg proteins, Aut2p/Apg4p, Apg7p and Aut1p/Apg3p (Ichimura *et al*., 2000; Kirisako *et al*., 2000). The C-terminal Arg117 of Aut7p is removed through the action of Aut2p, a cysteine protease (Kirisako *et al*., 2000), to expose Gly116. Following activation by Apg7p (E1), the processed Aut7p is transferred to Aut1p (E2). Aut7p is then covalently linked to PE. Aut2p further cleaves Aut7p–PE, releasing Aut7p, an essential step in the normal progression of autophagy (Kirisako *et al*., 2000). Aut7p is the first protein to localize to autophagosomes and intermediate structures (Kirisako *et al*., 1999; Huang *et al*., 2000); this characteristic of Aut7p allows us to use Aut7p to monitor autophagosome formation. LC3, the mammalian homologue of Aut7p, is

also localized on the membranes of autophagosomal and precursor membranes (Kabeya *et al*., 2000; Mizushima *et al*., 2001).

Additional Apg proteins, not known to participate in ubiquitin-like systems, are also required for autophagy. Vps30p/Apg6p, in addition to a role in autophagy, functions in vacuolar protein sorting (Kametaka *et al*., 1998). Vps30p forms a specific phosphatidylinositol 3-kinase (PI3-kinase) complex required for autophagy, consisting of Vps30p, Apg14p, Vps34p and Vps15p. These data suggest that the dynamic membrane events mediated by the PI3-kinase complex are necessary for autophagy (Kihara *et al*., 2001a). A class of PI3-kinase and beclin, a human homologue of Vps30p, are also essential for autophagy in human cells (Liang *et al*., 1999; Petiot *et al*., 2000). Beclin physically interacts with the PI3-kinase complex on the *trans*-Golgi network (Kihara *et al*., 2001b).

Tor kinase negatively regulates the induction of autophagy; this kinase activity is inhibited by rapamycin (Noda and Ohsumi, 1998). As the inactivation of Tor activity induces autophagy, treatment with rapamycin mimics the starvation response. The inactivation of Tor activity causes a rapid dephospholylation of Apg13p (Abeliovich *et al*., 2000; Kamada *et al*., 2000). Apg13p and Apg17p associate with Apg1p protein kinase (Matsuura *et al*., 1997) to form the Apg1p protein kinase complex, an essential component of autophagy. Binding of dephosphorylated Apg13p to this complex enhances the kinase activity of Apg1p (Kamada *et al*., 2000).

The characteristics of each Apg protein are gradually being uncovered; their functional interrelationship, however, is poorly understood. This is due to a lack of markers allowing the identification of intermediate steps occurring before or during autophagosome formation. To obtain further insights into the functional relationship between the Apg proteins, we observed the behaviour of Apg proteins fused to fluorescent proteins utilizing a sensitive imaging system. We examined the dynamics of the Apg proteins involved in the two ubiquitin-like systems, Apg5p and Aut7p. Based on their modification and localization in *apg* mutants, we have defined a pre-autophagosomal structure containing Apg1p, Apg2p, Apg5p, Aut7p and Apg16p. This structure, involved in the production of autophagosomes, provides a clue for investigating the steps of autophagosome formation.

Results

A punctate structure on which Apg1p, Apg5p, Aut7p and Apg16p are colocalized

Apg proteins are involved in several essential reactions in autophagy, such as ubiquitin-like systems or phosphorylation reactions. The interrelationship between these reactions in autophagosome formation, however, remains unknown. It is critical to know the intracellular localization. Several Apg proteins, e.g. Apg5p (George *et al*., 2000), Aut7p/Apg8p (Kim *et al*., 2001) and Apg9p (Noda *et al*., 2000), are localized to perivacuolar punctate structures. To analyse the localization of Apg proteins to these punctate structures, we visualized green fluorescent protein (GFP)-fused Apg proteins using a sensitive microscope system. GFP fusions were expressed from centromeric plasmids under the control of natural promoters. In Δ*aut7* cells expressing physiological levels of a GFP–Aut7p fusion protein (Figure 1A), GFP–Aut7p complemented the defect of autophagy (Figure 1C–E). These molecules were localized to punctate structures, proximal to the vacuole (Figure 1H and I). Apg5p–GFP retained the ability to conjugate with Apg12p (Figure 1B); when introduced into deficient cells, Apg5p–GFP restored proper autophagic function (Figure 1C, F and G). The

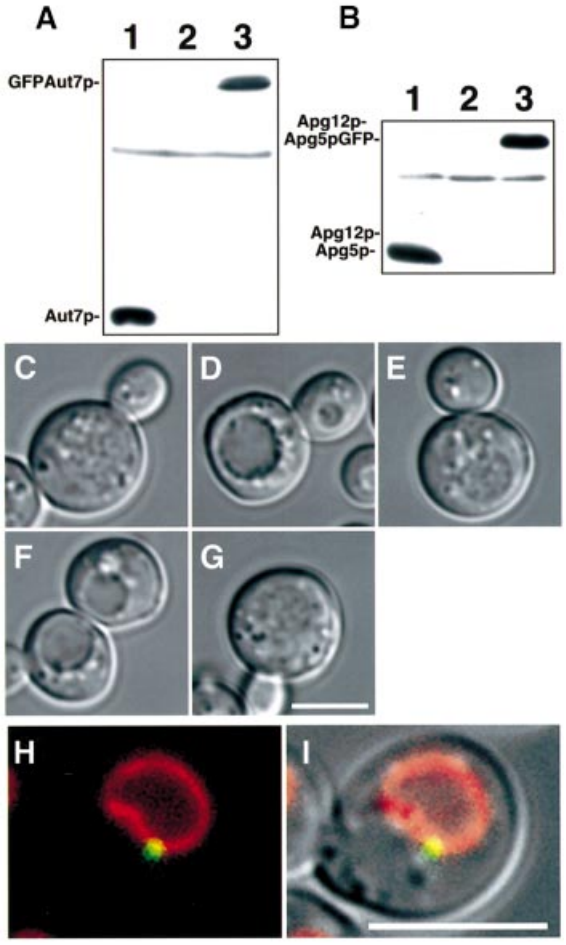

Fig. 1. Functional GFP–Aut7p and Apg5p–GFP are expressed from natural promoters at physiological levels. (**A**) The expression level of GFP–Aut7p under growing conditions. Cell lysates were prepared as described in Materials and methods. (1) Wild-type (KA311A), (2) Δ*aut7* (YYK218) and (3) Δ*aut7* (YYK218) expressing GFP–Aut7p. (**B**) The Apg12p–Apg5p conjugate was produced normally in Δ*apg5* cells expressing Apg5p–GFP. Cell lysates were prepared as described in Materials and methods. (1) Wild-type (KA311A), (2) Δ*apg5* (GYS59) and (3) Δ*apg5* (GYS59) expressing Apg5p–GFP. (**C**–**G**) The accumulation of autophagic bodies was examined under a light microscope. Cells were incubated for 6 h in 0.17% yeast nitrogen base w/o amino acid and ammonium sulfate containing 1 mM PMSF. Nomarski images of (C) wild-type (KA311A), (D) Δ*aut7* (YYK218), (E) Δ*aut7* (YYK218) expressing GFP–Aut7p, (F) Δ*apg5* (GYS59) and (G) Δ*apg5* (GYS59) expressing Apg5p–GFP. (H–I) GFP–Aut7p visualized in Δ*aut7* cells (KVY5) under growing conditions. A punctate structure containing GFP–Aut7p is detected close to the vacuole, identified by FM4-64 labelling. (**H**) Fluorescence of GFP–Aut7p (green) and a FM4-64-labelled vacuole (red). (**I**) The Nomarski image is overlaid with GFP–Aut7p and FM4-64 fluorescence. The punctate structures, close to the vacuole, were detected in 43 of 206 cells (21%). Bar: 5 μm.

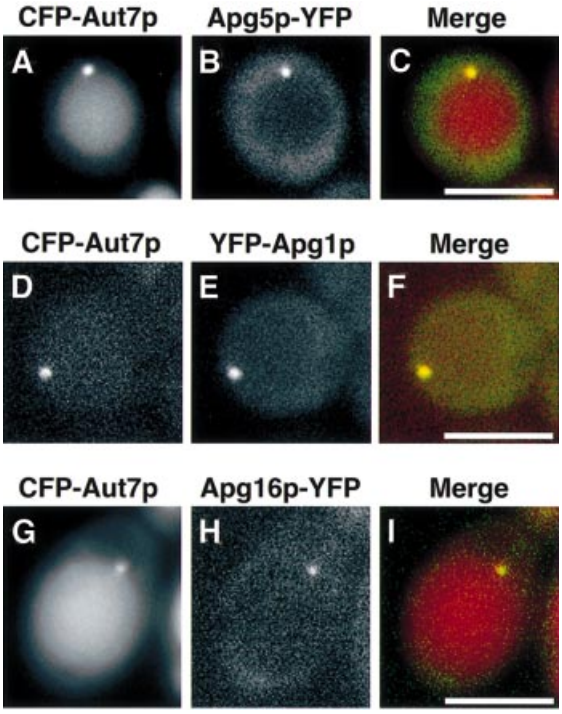

Fig. 2. Colocalization of Apg1p, Apg5p, Apg16p and Aut7p on a punctate structure close to the vacuole. (**A**–**C**) Δ*apg5* cells (YNM119) expressing Apg5p–YFP and CFP–Aut7p were treated with rapamycin for 3 h: (A) Apg5p–YFP, (B) CFP–Aut7p, (C) merged image of Apg5p–YFP (green) and CFP–Aut7p (red). (**D**–**F**) Δ*apg1* cells (NNY20) expressing CFP–Aut7p and YFP–Apg1p were treated with rapamycin for 30 min: (D) CFP–Aut7p, (E) YFP–Apg1p, (F) merged image of CFP–Aut7p (red) and YFP–Apg1p (green). (**G**–**I**) Δ*apg16* cells (KVY117) expressing CFP–Aut7p and YFP–Apg16p were treated with rapamycin for 6 h: (G) CFP–Aut7p, (H) YFP–Apg16p, (I) merged image of CFP–Aut7p (red) and YFP–Apg16p (green). Bar: 5 μm.

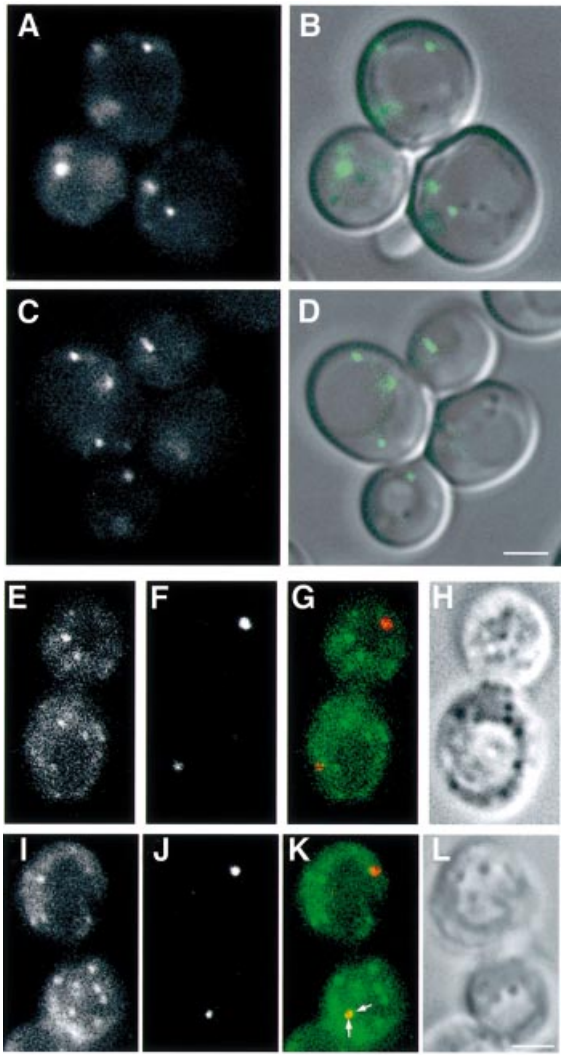

Fig. 3. Localization of Aut7p and Apg9p–GFP. (**A** and **B**) Apg9p–GFP was visualized in Δ*apg9* cells (CTD1) under growing conditions: (A) Apg9p–GFP, (B) the Nomarski image is overlaid with the fluorescence of Apg9p–GFP. (**C** and **D**) Apg9p–GFP in Δ*apg9*Δ*apg14* cells (GYS29) was identified under growing conditions: (C) Apg9p–GFP, (D) the Nomarski image is overlaid with the fluorescence of Apg9p–GFP. (**E**–**L**) Δ*apg9* cells (CTD1) expressing Apg9p–GFP were treated with rapamycin for 2 h. Immunofluorescence microscopy was performed as described in Materials and methods. (E and I) Apg9p–GFP, (F and J) Aut7p, (G and K) merged images of Apg9p–GFP (green) and Aut7p (red) and (H and L) Nomarski images. Apg9p and Aut7p were occasionally found in close proximity (arrows in K). Bar: 2 μm.

additional chimeric proteins used in this study were also functional in the autophagic process (data not shown).

Next, we fused cyan fluorescent protein (CFP) and yellow fluorescent protein (YFP) to several different Apg proteins and examined their colocalization. Fluorescent Aut7p served as a marker of the punctate structures. Apg1p, Apg5p and Apg16p colocalized with Aut7p on a single punctate structure located close to the vacuole (Figure 2). After the addition of rapamycin, CFP–Aut7p was delivered to vacuoles in a time-dependent manner (Figure 2A, D and G). YFP–Apg1p was delivered to vacuoles after lengthy treatment with rapamycin (data not shown), whereas Apg5p–YFP and Apg16p–YFP were never transported to vacuoles (Figure 2B and H). Apg2p colocalizes with Aut7p on a perivacuolar punctate structure (Shintani *et al*., 2001). Consequently, the punctate structure is shown to contain Apg1p, Apg2p, Apg5p, Aut7p and Apg16p. Apg12p is likely to be colocalized with Apg5p and Apg16p as a component of the AApg12p–Apg5p–Apg16p complex. As Apg13p and Apg17p interact physically with Apg1p (Kamada *et al*., 2000), it is probable that these molecules also reside on the punctate structure. This is the first report demonstrating the colocalization of multiple Apg proteins.

Apg9p is a putative membrane protein and is not cofractionated with typical endomembrane marker proteins, autophagosomes or Cvt vesicles (Noda *et al*., 2000). Apg9p–GFP exhibited an uneven, cytosolic distribution in addition to its localization on several punctate structures (Noda *et al*., 2000; Figure 3A and B). This pattern was not altered in other *apg* mutants (Figure 3C and D; data not shown). To examine the use of this protein as a punctate structure marker, we compared the localization of Apg9p–GFP and Aut7p by immunofluorescence microscopy. The punctate structures labelled with Aut7p seldom colocalized with those labelled by Apg9p–GFP (Figure 3E–L), although the two structures were occasionally in close proximity (arrows in Figure 3K). This pattern of Apg9p indicates that it is not a suitable marker for the punctate structure.

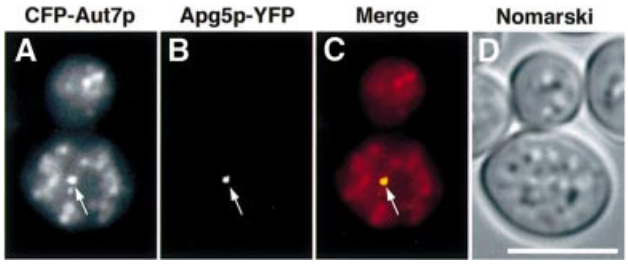

Fig. 4. Localization of Aut7p and Apg5p in Δ*ypt7* cells. Δ*ypt7*Δ*apg5* cells (YAK3) expressing CFP–Aut7p and Apg5p–YFP were treated with rapamycin for 5 h. (**A**) Autophagosomes stained with CFP–Aut7p; (**B**) Apg5p–YFP; (**C**) merged image of CFP–Aut7p (red) and Apg5p–YFP (green); (**D**) Nomarski image: CFP–Aut7p and Apg5p–YFP colocalized on a punctate structure (arrows). Bar: 5 μm.

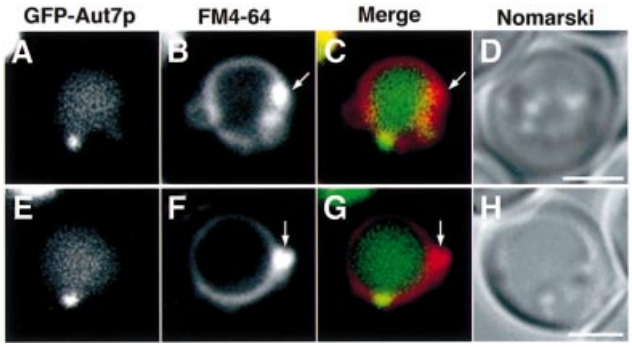

Fig. 5. Localization of Aut7p and the class E compartment. The class E compartment of Δ*vps4* cells (MBY3) expressing GFP–Aut7p was labelled with FM4-64 as described in Materials and methods, following treatment with rapamycin for 2 h. (**A** and **E**) GFP–Aut7p. (**B** and **F**) The class E compartments stained with FM4-64 (arrows). (**C** and **G**) Merged images of GFP–Aut7p (green) and FM4-64 (red). (**D** and **H**) Nomarski images. Bar: 2 μm.

Electron microscopic analysis established that autophagosomes accumulate in the Δ*ypt7* mutant (Kirisako *et al*., 1999). We therefore examined the localization of Apg5p–YFP and CFP–Aut7p in Δ*ypt7* cells. Following rapamycin treatment of these cells, autophagosomes labelled with CFP–Aut7p appeared as dim dots in the cytosol (Figure 4A), whereas Apg5p–YFP was detected as a punctate pattern (arrow in Figure 4B). Every punctate structure labelled with Apg5p–YFP was associated with CFP–Aut7p (arrow in Figure 4C). CFP–Aut7p staining of the structure was of a greater intensity than the other CFP–Aut7p dots (arrow in Figure 4A). These observations suggest that this punctate structure containing several colocalized Apg proteins is not an autophagosome.

To investigate the involvement of the endocytic pathway in punctate structure formation, we examined the class E compartment, an exaggerated prevacuolar compartment in class E vacuolar protein sorting (*vps*) mutants (Raymond *et al*., 1992). The class E compartment is labelled with FM4-64, a lipophilic stylyl dye, as an intensely stained membrane-enclosed structure (Vida and Emr, 1995) and morphologically similar to the punctate structure labelled with Aut7p. We observed the localization of GFP–Aut7p in a class E *vps* mutant, Δ*vps4* (Raymond *et al*., 1992). The GFP–Aut7p punctate structure did not colocalize with the class E compartment in this mutant (Figure 5). These data suggest that the punctate structure is not organized through the endocytic pathway. Therefore, this punctate structure is a novel structure localized proximal to the vacuole.

Genetic analysis of APG genes required for the organization of the punctate structure

We have found a novel punctate structure in which at least five Apg proteins are concentrated. We examined the organization within this punctate structure by studying the localization of Apg5p–GFP and GFP–Aut7p in *apg* mutants (Figure 6; summarized in Table I). We also assessed the quantities of PE-conjugated Aut7p (Ichimura *et al*., 2000; Kirisako *et al*., 2000) in each *apg* mutant by SDS–PAGE in the presence of 6 M urea (Figure 7). Based on these observations, we grouped the *apg* mutants into three categories. These classes corresponded well to defined functional units, including the Apg1p protein kinase complex, the two ubiquitin-like systems and the PI3-kinase complex necessary for autophagy. This classification provides several new insights into the interaction between these classes, detailed in the following sections.

Analyses of class A apg mutants provide evidence that the punctate structure is involved in autophagosome formation

The class A mutants possess both Apg5p–GFP and GFP–Aut7p localized to the punctate structure as in wild-type cells (Table I). The class A genes consist of *APG1*, *APG2*, *APG13* and *APG17*. Apg13p and Apg17p are regulatory factors of the Apg1p protein kinase. As the class A mutants demonstrate normal punctate structures, the Apg1p protein kinase complex is unlikely to be involved in the formation of the punctate structure. The class A mutants all possessed normal levels of Aut7p–PE (Figure 7).

To examine whether the punctate structure is physiologically functional, we generated an *apg1*^{ts} allele by polymerase chain reaction (PCR) mutagenesis. Autophagic activities were measured by monitoring the alkaline phosphatase (ALP) activity in cells expressing a cytosolic proform of the ALP (Pho8Δ60p), which is transported to vacuoles and becomes mature (Noda *et al*., 1995). We estimated the temperature sensitivity of this allele from the maturation of API (Figure 8A) and the ALP assay (Figure 8B) using Δ*apg1* cells carrying the apg1^{ts} plasmid (*apg1*^{ts} cells). At 23°C, the *apg1*^{ts} cells contained normal levels of mature API (Figure 8A) and possessed significant autophagic activity (Figure 8B). At 37°C, however, both the maturation of API and autophagic activity were completely blocked (Figure 8A and B). Autophagy in the *apg1*^{ts} cells at 30°C occurred at the same levels as at 23°C. The activity of ALP increased linearly with time for 6 h following incubation in nitrogen-free medium at 23°C (Figure 8C). On transferring the cells to 37°C, autophagy was immediately blocked (Figure 8C). When the cells were transferred from 37°C to 23°C, the autophagic activity was recovered without a lag period (Figure 8C). Apg1^{ts}p was detectable by immunoblot even after an overnight incubation at 37°C (Figure 8A), demonstrating that *apg1*^{ts} is a reversible temperature-sensitive allele defective in autophagy.

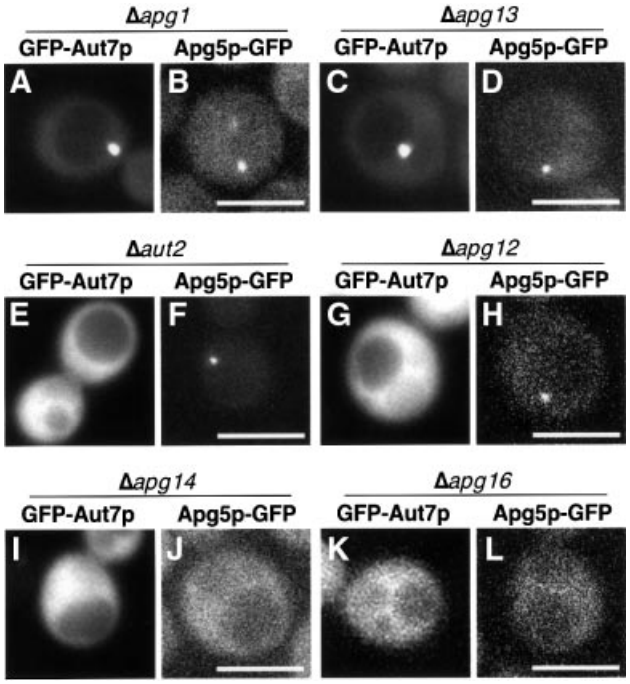

Fig. 6. Localization of GFP–Aut7p and Apg5p–GFP in the *apg* mutants grown in SD + CA medium. (**A**) Δ*apg1* cells (NNY20). GFP–Aut7p was detected on a punctate structure close to the vacuole in 30 of 161 cells (18%). Δ*apg13* (**C**; TFD13W2), Δ*apg17* (YYK111), *apg2* (MT2-4-4) cells exhibited an identical phenotype. (**B**) Δ*apg1* cells (YYK36) expressing Apg5p–GFP. Punctate structures were detected in 11 of 91 cells (12%). Δ*apg13* (**D**; TFD13W2), Δ*apg17* (YYK111) and *apg2* (MT2-4-4) cells demonstrated an identical phenotype. (**E**) This image of a Δ*aut2* cell (GYS6) expressing GFP–Aut7p is representative of the Aut7 system. The punctate structures were detected in one of 78 cells (1%). Δ*apg7* (GYS9) and Δ*aut1* (GYS5) cells exhibited the same phenotype. (**F**) Δ*aut2* cells (GYS6) expressing Apg5p–GFP. A single punctate structure was detected in 11 of 52 cells (21%). Δ*aut1* (GYS5) and Δ*aut7* (YYK218) cells demonstrated a similar phenotype. (**G**) This Δ*apg12* cell (GYS13) expressing GFP–Aut7p is representative of mutants of the Apg12 system. Punctate structures were detected in one of 84 cells (1%). Δ*apg10* (TFD10-L1) and Δ*apg5* (SKD5-1D) cells possessed an identical phenotype. (**H**) A Δ*apg5*Δ*apg12* cell (YNM117) expressing Apg5p–GFP. A single punctate structure was detected in 16 of 104 cells (15%). Δ*apg7* (GYS9), Δ*apg10* (TFD10-L1) and Δ*apg5* (SKD5-1D) cells all exhibited an identical phenotype. (**I**) A Δ*apg14* cell (SKD14–1C) expressing GFP–Aut7p. None of the 51 cells displayed a punctate structure. Δ*vps30* cells (SKD6-1D) and Δ*apg9* cells (CTD1) possessed an identical phenotype. (**J**) A Δ*apg14* cell (AKY12) expressing Apg5p–GFP under growing conditions. Punctate structures were observed in one of 248 cells (<1%). Δ*vps30* cells (AKY74) and Δ*apg9* cells (CTD1) exhibited an identical phenotype. (**K**) A Δ*apg16* cell (KVY117) expressing GFP–Aut7p. No punctate structures were observed in any of the 77 cells. (**L**) A Δ*apg5*Δ*apg16* cell (YNM126) expressing Apg5p–GFP under growing conditions. No punctate structures were observed in the 184 cells examined. Bar: 5 μm.

Table I. Localization of GFP–Aut7p and Apg5p–GFP on the punctate structure in *apg* mutants

Genotype	GFP–Aut7p	Apg5p–GFP
Δ*apg1*	+	+
apg2	+	+
Δ*aut1*/Δ*apg3*	–	+
Δ*aut2*/Δ*apg4*	–	+
Δ*apg5*	–	+ (WT)
Δ*vps30*/Δ*apg6*	–	–
Δ*apg7*	–	+
Δ*aut7*/Δ*apg8*	+ (WT)	+
Δ*apg9*	–	–
Δ*apg10*	–	+
Δ*apg12*	–	+
Δ*apg13*	+	+
Δ*apg14*	–	–
Δ*apg16*	–	–
Δ*apg17*	+	+
Δ*apg1*Δ*apg7*	–	not examined
Δ*apg1*Δ*vps30*	–	not examined
Δ*apg1*Δ*apg9*	–	not examined
Δ*aut2*Δ*apg10* expressing GFP–Aut7FGp	–	not examined
Δ*aut2*Δ*apg12* expressing GFP–Aut7FGp	–	not examined
Δ*vps38*	+	not examined

+: GFP–Aut7p or Apg5p–GFP is localized to the punctate structure.
–: GFP–Aut7p or Apg5p–GFP shows a diffuse cytoplasmic staining pattern.
WT: wild type.

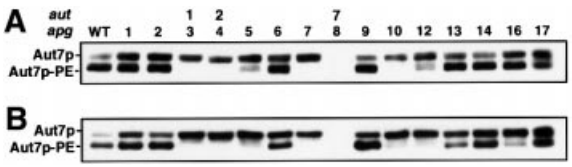

Fig. 7. Levels of Aut7p–PE present in each *apg* mutant. Lysates were prepared by glass bead disruption prior to SDS–PAGE as described in Materials and methods. (**A**) Cells in vegetative growth. (**B**) Cells following a 4.5 h starvation in SD (–N) medium. We examined the phenotype of wild type (SEY6210), Δ*apg1* (GYS102), *apg2* (MT2-4-4), Δ*aut1* (KVY113), Δ*aut2* (KVY13), Δ*apg5* (KVY142), Δ*vps30* (KVY135), Δ*apg7* (KVY118), Δ*aut7* (KVY5), Δ*apg9* (KVY114), Δ*apg10* (KVY136), Δ*apg12* (KVY115), ΔΔ*apg13* (KVY116), Δ*apg14* (GYS115), Δ*apg16* (KVY117) and Δ*apg17* (YYK111) cells.

On shifting the temperature from 37°C to 30°C, we followed the dynamics of GFP–Aut7p in *apg1*^{ts} cells. At 30°C, GFP–Aut7p was visualized in the punctate structure and the vacuole after rapamycin treatment, as seen in wild-type cells (Figure 9A). At 37°C, the staining intensity of the punctate structure increased, accompanied by a lack of vacuolar staining after rapamycin treatment (Figure 9B, 4 min). Next, we examined the progression of GFP–Aut7p staining following temperature decrease in real time using time-lapse microscopy. Within 10 min, several dots labelled with GFP–Aut7p separated from the punctate structure (Figure 9B). During 30 min of incubation at 30°C, fluorescence intensity of vacuoles became brighter as these dots disappeared, suggesting that they are autophagosomes. We concluded that the punctate structure actually participates in the formation of autophagosomes.

We next treated *apg1*^{ts} cells with cycloheximide for 20 min, following a 4 h incubation at 37°C in the presence of rapamycin. On decreasing the temperature, similar dots appeared, leading to fluorescent staining of the vacuole (data not shown). This experiment demonstrates that the emergence of autophagosomes from the punctate structure depends on the activity of Apg1p; *de novo* protein synthesis, however, is not necessary. As Apg1p is localized to the punctate structure (Figure 2D–F), the Apg1p protein kinase complex functions in autophagosome formation at a later step than the organization of the structure. We therefore designated this punctate structure the 'pre-autophagosomal structure'.

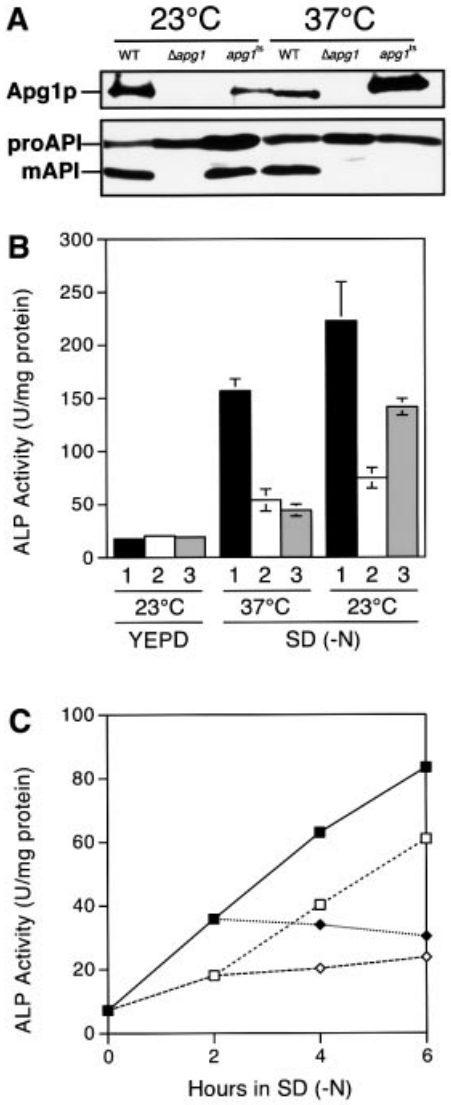

Fig. 8. *apg1*^{ts} mutant possessing functional temperature sensitivity. (**A**) Although temperature-sensitive Apg1p was detectable, the maturation of API was completely blocked at 37°C in *apg1*^{ts} cells. The API proform (proAPI) is processed to mature API (mAPI) in an Apg1p activity-dependent manner. Wild-type cells (TN125), Δ*apg1* cells (YYK126) and Δ*apg1* cells (YYK126) carrying the apg1^{ts} plasmid were grown in YEPD medium at 23°C or 37°C overnight. Apg1p and API were detected as described in Materials and methods. (**B**) Δ*apg1* cells (YYK126) carrying (1) the APG1 plasmid, (2) the vector or (3) the apg1^{ts} plasmid were grown in YEPD medium at 23°C. They were then transferred into SD (–N) medium at 23°C or 37°C and incubated for 6 h before ALP activity was measured. (**C**) Δ*apg1* cells (YYK126) carrying the apg1^{ts} plasmid were grown in YEPD medium at 23°C. The cells were then transferred into SD (–N) medium and incubated at 23°C or 37°C. Closed squares, cells starved continuously at 23°C. Open squares, cells incubated for 2 h at 23°C and then transferred to 37°C. Open lozenges, cells starved continuously at 37°C. Closed lozenges, cells incubated for 2 h at 37°C and then transferred to 23°C.

Class B apg mutants have a defect in the localization of Aut7p on the pre-autophagosomal structure

In class B mutants Δ*aut1*, Δ*aut2*, Δ*apg5*, Δ*apg7*, Δ*apg10* and Δ*apg12*, Apg5p–GFP was detected on the pre-autophagosomal structure; GFP–Aut7p was not. Interestingly, these are the genes involved in the two ubiquitin-like conjugation systems: the Aut7 system (Δ*aut2*, Δ*apg7*

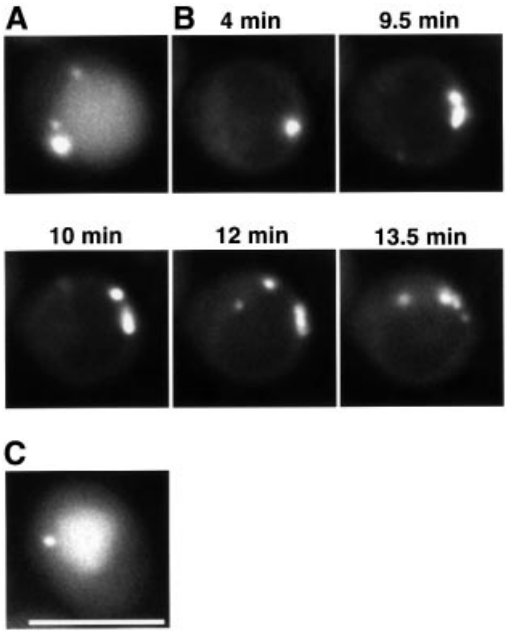

Fig. 9. Time-lapse microscopy of *apg1*^{ts} cells expressing GFP–Aut7p. Δ*apg1* cells (NNY20) carrying the apg1^{ts} and GFP–Aut7p plasmids were used. (**A**) Cells treated with rapamycin for 3 h at 30°C. (**B**) Time-lapse images following temperature decrease. Cells were treated with rapamycin for 4 h at 37°C before decreasing the temperature to 30°C. (**C**) Cell incubated for 2 h at 30°C after temperature decrease. Bar: 5 μm.

and Δ*aut1*) and the Apg12p–Apg5p conjugation system (Δ*apg12*, Δ*apg7*, Δ*apg10* and Δ*apg5*). In the Δ*apg1*Δ*apg7* double mutant, GFP–Aut7p did not localize to the pre-autophagosomal structure (Table I). This result demonstrates that *APG7* (class B) is epistatic to *APG1* (class A) for the localization of Aut7p, suggesting that the class B *APG* genes govern the localization of Aut7p to the pre-autophagosomal structure prior to class A gene function. As previously reported, mutants of the Aut7 system lacked detectable Aut7p–PE (Figure 7; Ichimura *et al.*, 2000). These studies demonstrated that the localization of GFP–Aut7p to the pre-autophagosomal structure is tightly coupled to Aut7p lipidation. The association of Aut7p with the pre-autophagosomal structure occurs with the PE-conjugated form. In Δ*aut1* or Δ*aut2* mutant, the Apg12p–Apg5p conjugate is formed normally (Mizushima *et al.*, 1998); Apg5p–GFP was localized on the pre-autophagosomal structure, as seen in wild-type cells (Table I). Therefore, the lipidation of Aut7p is essential for the localization of Aut7p, but not required for localization of (Apg12p–)Apg5p to the pre-autophagosomal structure.

Interestingly, Apg5p–GFP was detected on the pre-autophagosomal structure in mutants of the Apg12 system (Δ*apg12* and Δ*apg10*; Table I), suggesting that the conjugation of Apg12p is not necessary for Apg5p localization. In Apg12 system mutants (Δ*apg12*, Δ*apg10* and Δ*apg5*), we could not detect GFP–Aut7p on the pre-autophagosomal structure (Table I). In addition, these mutants demonstrated severely reduced levels of Aut7p–PE (Figure 7). A defect in the membrane association of Aut7p in Apg12p conjugation mutants (Kim *et al.*, 2001) may be explained by decreases in the total level of Aut7p–PE in the absence of the conjugate.

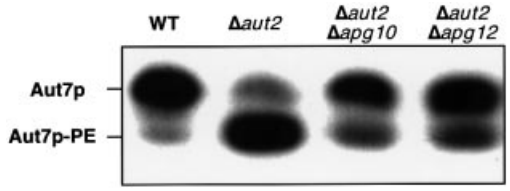

Fig. 10. Amounts of Aut7p–PE in Δ*aut2* cells expressing Aut7FGp during vegetative growth. Lysates were prepared by glass bead disruption and subjected to SDS–PAGE as described in Materials and methods. The strains used in this experiment are as follows: wild type (SEY6210), Δ*aut2* (KVY13), Δ*aut2*Δ*apg10* (KVY150) and Δ*aut2*Δ*apg12* (KVY148).

To examine the effects of the disruption of the Apg12p–Apg5p conjugate on Aut7p localization, we estimated the levels of Aut7p–PE in Δ*aut2* cells expressing the carboxy-terminal processed form of Aut7p (Aut7FGp; Ichimura *et al*., 2000; Kirisako *et al*., 2000). Aut2p/Apg4p, a cysteine protease, is essential for Aut7p processing and Aut7p–PE deconjugation. Aut7p–PE accumulates in Δ*aut2* cells expressing Aut7FGp because of the inability of these cells to deconjugate Aut7p–PE (Kirisako *et al*., 2000). The levels of Aut7p–PE in Δ*aut2*Δ*apg10* and Δ*aut2*Δ*apg12* cells were reduced from the levels in Δ*aut2* cells, but Aut7p–PE was actually generated in Δ*aut2*Δ*apg10* and Δ*aut2*Δ*apg12* cells (Figure 10). This result indicates the Apg12p–Apg5p conjugate is not essential for Aut7p–PE formation. We then constructed a GFP–Aut7FG plasmid, which we expressed in Δ*aut2*Δ*apg10* and Δ*aut2*Δ*apg12* cells. Although significant amounts of Aut7p–PE were produced in these mutants (Figure 10), GFP–Aut7FGp did not localize to the pre-autophagosomal structure (Table I). This result indicates that the Apg12p–Apg5p conjugate is absolutely required for the proper localization of Aut7p. The role of the conjugate is not restricted to the localization of Aut7p, however, as Δ*apg5* cells possess more severe defects in API maturation than the Δ*aut7* cells (Abeliovich *et al*., 1999, 2000).

Class C apg mutants do not deliver either Apg5p or Aut7p to the pre-autophagosomal structure

In class C mutants, Δ*vps30*, Δ*apg9*, Δ*apg14* and Δ*apg16*, neither Apg5p–GFP nor GFP–Aut7p localized to the pre-autophagosomal structure. *VPS30* and *APG14* are the genes involved in the autophagy-specific PI3-kinase complex. Double disruptant Δ*apg1*Δ*vps30* or Δ*apg1*-Δ*apg9*, expressing GFP–Aut7p demonstrated a diffuse cytoplasmic staining pattern (Table I). This result indicates that *VPS30* and *APG9* (class C) are epistatic to *APG1* (class A) in the organization of the pre-autophagosomal structure. Therefore, the class C *APG* genes play roles in the organization of Apg5p and Aut7p on the pre-autophagosomal structure in a class A gene-independent manner. We further analysed the levels of Aut7p–PE in these mutants. Δ*apg16* cells contained significant levels of Aut7p–PE during vegetative growth (Figure 7A). The ratio of Aut7p–PE to unmodified Aut7p, however, decreased after nitrogen starvation (Figure 7B). The levels of Aut7p–PE in growing cells and starved cells were similar (data not shown), indicating that the synthesis of Aut7p during starvation resulted in a decrease in the relative levels of Aut7p–PE in Δ*apg16* cells. In contrast, Δ*vps30*, Δ*apg9*, Δ*apg14* cells possessed normal levels of Aut7p–PE, regardless of the nutrient conditions (Figure 7).

Apg16p is a coiled-coil protein linking the Apg12p–Apg5p conjugates (Mizushima *et al*., 1999). Although the Apg12p–Apg5p conjugate was formed, we did not observe a dot structure of Apg5p–GFP in Δ*apg16* cells (Table I). This observation suggests that the interaction of Apg5p and Apg16p is necessary for the proper localization of Apg5p to the pre-autophagosomal structure. Although Aut7p–PE was formed in the Δ*apg16* mutant during vegetative growth (Figure 7A), we could not observe the localization of Aut7p to the pre-autophagosomal structure (Table I). This phenotype is similar to that of Δ*aut2*-Δ*apg10* or Δ*aut2*Δ*apg12* cells expressing GFP–Aut7FGp (Table I), which contain significant levels of Aut7p–PE (Figure 10). This result indicates that Apg12p–Apg5p–Apg16p complex formation is needed for the localization of Aut7p. As the Δ*apg16* mutant failed to maintain Aut7p–PE levels during starvation, the Apg12p–Apg5p–Apg16p complex must be necessary for the maintenance of Aut7p–PE levels.

Two types of PI3-kinase complex contain Vps34p, Vps15p and Vps30p/Apg6p as common components (Kihara *et al*., 2001a). In these complexes, Apg14p and Vps38p are the components specifying autophagy or the carboxypeptidase Y (CPY), a vacuolar resident enzyme, sorting pathway, respectively. In Δ*apg14* cells, Aut7p and Apg5p were located diffusely throughout the cytoplasm, whereas in Δ*vps38* cells, the pre-autophagosomal structure was detectable (Table I). In Δ*vps30* and Δ*apg14* strains, Aut7p–PE and the Apg12p–Apg5p conjugate were produced normally (Figure 7; Mizushima *et al*., 1998). These results indicate that the autophagy-specific PI3-kinase complex is essential to recruit Aut7p–PE and the Apg12p–Apg5p conjugate to the pre-autophagosomal structure. The Δ*apg9* mutant also demonstrates class C phenotype. A physical interaction of Apg9p with other Apg proteins, however, has not been identified. Our results suggest that Apg9p has some relationship with the autophagy-specific PI3-kinase complex.

Discussion

We and other groups have reported the intracellular localization of several Apg proteins forming a punctate structure close to the vacuole. The physiological significance of this punctate structure, however, has not been examined in detail. Here, we systematically investigated the localization of GFP-tagged Apg proteins when expressed at physiological levels. These analyses identified a novel 'pre-autophagosomal structure', in which Apg1p, Apg2p, Apg5p, Aut7p and Apg16p are assembled. Apg5p and Aut7p are recruited to the structure by the action of Apg16p and the autophagy-specific PI3-kinase complex. The Apg1p protein kinase complex is also localized to the structure. This kinase functions in concert with the Apg12p–Apg5p–Apg16p complex and Aut7p to play a crucial role in generating autophagosomes. Our characterization of this structure found that Apg proteins exist in three functional groups, the Apg1p protein kinase complex, the ubiquitin-like systems (the Apg12 system

and the Aut7 system) and the autophagy-specific PI3-kinase complex. Epistatic analyses of the *apg* mutant phenotypes clearly uncovered the interrelationship on the pre-autophagosomal structure between these three groups. Although the functions of the *APG2* and *APG9* genes remain unknown, we obtained results suggesting that these genes encode proteins acting close to the Apg1p protein kinase complex and the autophagy-specific PI3-kinase complex, respectively.

The pre-autophagosomal structure

Following rapamycin treatment, the fluorescence of GFP–Aut7p and other GFP-fused Apg proteins visualizing the pre-autophagosomal structure rapidly increases in intensity (data not shown). The amount of Aut7p increases during autophagy, whereas there is no significant increase in Apg1p, Apg2p, Apg5p or Apg16p. These results suggest the further recruitment of Apg proteins to the pre-autophagosomal structure by unknown mechanisms. This change in the composition of the pre-autophagosomal structure may initiate autophagosome formation.

Repeated cell fractionation analyses of Apg proteins have not uncovered a biochemical identification of the pre-autophagosomal fraction. It is likely that low levels of each Apg protein are recruited onto the structure; in addition, the structure may be unstable in cell lysates, leading to difficulties in its biochemical characterization. Aut7p is concentrated on premature autophagosomes, isolation membranes and Aut7p-enriched regions near the vacuole, as determined by immunoelectron microscopy (Kirisako *et al*., 1999). This Aut7p-enriched region is one candidate for the pre-autophagosomal structure. Our intensive examination of Aut7p-concentrated structures, however, has not succeeded in identifying a definite membrane structure corresponding to the pre-autophagosomal structure. The structure may not be observable under an electron microscope as a defined membrane compartment. At present, our analyses, based on fluorescence microscopy, are the most promising investigations dissecting the process of autophagosome formation.

We demonstrated that the pre-autophagosomal structure is a functional structure rather than a dead-end structure. Temperature shift experiments using the *apg1*^{ts} strain indicated that several dots separated from the pre-autophagosomal structure at a permissive temperature (Figure 9B) to subsequently stain the vacuole (Figure 9C). This result indicates that the pre-autophagosomal structure is an organizing centre for autophagosomes. Each dot corresponds to the pre-autophagosomal structure or an autophagosome; the weakly stained dots seen in later stages (12 min and 13.5 min in Figure 9B) may be autophagosomes.

The organization of the pre-autophagosomal structure is not affected in the class A mutants, Δ*apg1*, *apg2*, Δ*apg13* or Δ*apg17*. Furthermore, we demonstrated that Apg1p is a component of the pre-autophagosomal structure (Figure 2D–F). Apg13p and Apg17p are also likely components of the structure, as Apg1p interacts directly with Apg13p and Apg17p (Kamada *et al*., 2000). In response to nutrient depletion, enhanced activity of the Apg1p kinase complex controls switching from Cvt vesicle formation to autophagosome formation. Aut7p is normally induced in Δ*apg1* cells by rapamycin or starvation (Kirisako *et al*., 1999). Therefore, the Apg1p kinase complex plays a role in both the induction of autophagy and the initiation of autophagosome formation. The delivery of GFP–Apg1p to the vacuolar lumen during rapamycin treatment (data not shown) also supports the involvement of Apg1p in the latter stage of autophagosome formation.

Organization of the pre-autophagosomal structure

Aut7p–PE is an essential component of the pre-autophagosomal structure (Table I and Figure 7). We demonstrated that the absence of the Apg12p–Apg5p conjugate results in a severe decrease in Aut7p–PE levels (Figure 7). GFP–Aut7FGp is not detected on the pre-autophagosomal structure in Δ*aut2*Δ*apg10*, Δ*aut2*Δ*apg12* cells (Table I) despite significant levels of Aut7p–PE (Figure 10). These data suggest that the Apg12p–Apg5p conjugate must play a role in the localization of Aut7p–PE. On treatment with rapamycin, however, Δ*aut7* cells demonstrate some degree of API maturation, whereas Δ*apg5* cells possess no mature API (Abeliovich *et al*., 1999, 2000; Kirisako *et al*., 2000). This suggests that the conjugate is essential for both autophagosome formation and the maintenance of Aut7p–PE localized to the pre-autophagosomal structure.

Apg16p forms a complex with the Apg12p–Apg5p conjugate (Mizushima *et al*., 1999). GFP–Aut7p exhibits a diffuse staining pattern in Δ*apg16* cells, regardless of the normal levels of Aut7p–PE present during vegetative growth (Figure 7A). Δ*apg16* mutant failed to increase the level of Aut7p–PE during starvation (Figure 7B). Apg16p may participate in the maintenance of the Aut7p–PE levels during starvation. Apg5p–GFP also possesses a diffuse pattern throughout the cytosol in Δ*apg16* cells (Figure 6L). The localization of Apg16p to the structure (Figure 2G–I) suggests that Apg16p plays a role in targeting the AApg12p–Apg5p conjugate to the pre-autophagosomal structure. In Δ*apg16* cells, Aut7p–PE may not be localized on the pre-autophagosomal structure due to a lack of the AApg12p–Apg5p-Apg16p complex.

We could not identify GFP–Aut7p punctate structures in growing Δ*apg9* cells (Table I); the punctate structures are reported in Δ*apg9* cells under nitrogen-starved conditions (Kim *et al*., 2001). To investigate the localization of GFP–Aut7p during autophagy, we examined GFP–Aut7p in rapamycin-treated Δ*apg9* cells. We observed a similar punctate staining pattern similar to that described by Kim *et al*. (2001; data not shown). These punctate structures, however, were less distinct and of a lower intensity than those seen in Δ*apg1* cells (data not shown). This result suggests that Apg9p plays an important role in the recruitment of Aut7p to the pre-autophagosomal structure.

The autophagy-specific PI3-kinase complex controls the organization of the pre-autophagosomal structure but the PI3-kinase complex specific to the CPY pathway does not. In autophagy-specific PI3-kinase complex mutants, both Aut7p–PE and the Apg12p–Apg5p conjugate are produced normally, indicating that these conjugation reactions occur in the absence of the complex. One possible function of the autophagy-specific PI3-kinase complex is to select cargo during vesicle budding (Kihara *et al*., 2001a). The complex may load Aut7p–PE and/or the Apg12p–Apg5p conjugate into vesicles to facilitate their transport to the pre-autophagosomal structure. A second possibility is that

Table II. Strains used in this study

Strain	Genotype	Source
SEY6210	*MAT*α *ura3 leu2 his3 trp1 lys2 suc2*	Darsow *et al*. (1997)
YW5-1B	*MAT***a** *ura3 leu2 trp1*	Tsukada and Ohsumi (1993)
KA311A	*MAT***a** *ura3 leu2 his3 trp1*	K.Irie (Osaka University, Japan)
KA311B	*MAT*α Δ*ura3 leu2 his3 trp1*	K.Irie (Osaka University, Japan)
BJ2168	*MAT***a** *ura3 leu2 trp1 pep4-3 prb1-1122 prc1-407*	Yeast Genetic Stock Center
TN125	*MAT***a** *ade2 ura3 leu2 his3 trp1 lys2 pho8::pho8Δ60*	Noda and Ohsumi (1998)
GYS102	SEY6210 Δ*apg1::LEU2*	this study
MT2-4-4	*MAT*α Δ*leu2 ura3 apg2*	Tsukada and Ohsumi (1993)
KVY113	SEY6210 Δ*aut1::LEU2*	this study
KVY13	SEY6210 Δ*aut2::LEU2*	Kirisako *et al*. (2000)
KVY142	SEY6210 Δ*apg5::LEU2*	this study
KVY135	SEY6210 Δ*vps30::LEU2*	Kirisako *et al*. (2000)
KVY118	SEY6210 Δ*apg7::HIS3*	Kirisako *et al*. (2000)
KVY5	SEY6210 Δ*aut7::HIS3*	Kirisako *et al*. (1999)
KVY114	SEY6210 Δ*apg9::TRP1*	this study
KVY136	SEY6210 Δ*apg10::HIS3*	this study
KVY115	SEY6210 Δ*apg12::HIS3*	this study
KVY116	SEY6210 Δ*apg13::TRP1*	this study
GYS115	SEY6210 Δ*apg14::LEU2*	this study
KVY117	SEY6210 Δ*apg16::LEU2*	this study
NNY20	YW5-1B Δ*apg1::LEU2*	Matsuura *et al*. (1997)
GYS5	YW5-1B Δ*aut1::TRP1*	Ichimura *et al*. (2000)
GYS6	YW5-1B Δ*aut2::LEU2*	Ichimura *et al*. (2000)
SKD5-1D	YW5-1B Δ*apg5::LEU2*	Kametaka *et al*. (1996)
SKD6-1D	YW5-1B Δ*vps30::LEU2*	Kametaka *et al*. (1998)
GYS9	YW5-1B Δ*apg7::LEU2*	Ichimura *et al*. (2000)
CTD1	YW5-1B Δ*apg9::TRP1*	Noda *et al*. (2000)
TFD10-L1	YW5-1B Δ*apg10::LEU2*	Shintani *et al*. (1999)
GYS13	YW5-1B Δ*apg12::TRP1*	this study
TFD13W2	YW5-1B Δ*apg13::TRP1*	Funakoshi *et al*. (1997)
SKD14–1C	YW5-1B Δ*apg14::LEU2*	Kametaka *et al*. (1998)
YYK36	KA311A Δ*apg1::LEU2*	Kamada *et al*. (2000)
GYS59	KA311A Δ*apg5::HIS3*	this study
YNM119	KA311B Δ*apg5::HIS3*	Mizushima *et al*. (1998)
AKY74	KA311A Δ*vps30::LEU2*	this study
YYK218	KA311A Δ*aut7::TRP1*	this study
AKY12	KA311A Δ*apg14::LEU2*	this study
YYK111	KA311A Δ*apg17::HIS3*	Kamada *et al*. (2000)
YYK190	BJ2168 Δ*apg1::LEU2*	this study
YYK126	TN125 Δ*apg1::LEU2*	Kamada *et al*. (2000)
YAK3	SEY6210 Δ*ypt7::HIS3* Δ*apg5::LEU2*	this study
MBY3	SEY6210 Δ*vps4::TRP1*	Babst *et al*. (1997)
YNM117	*MAT***a** *ura3 leu2 trp1* Δ*apg5::LEU2* Δ*apg12::HIS3*	Mizushima *et al*. (1999)
YNM126	KA311B Δ*apg5::HIS3* Δ*apg16::LEU2*	Mizushima *et al*. (1998)
GYS22	YW5-1B Δ*apg1::LEU2* Δ*apg7::HIS3*	this study
GYS23	YW5-1B Δ*apg1::URA3* Δ*vps30::LEU2*	this study
GYS24	YW5-1B Δ*apg1::LEU2* Δ*apg9::TRP1*	this study
GYS29	YW5-1B Δ*apg9::TRP1* Δ*apg14::LEU2*	this study
KVY150	SEY6210 Δ*apg4::LEU2* Δ*apg10::HIS3*	this study
KVY148	SEY6210 Δ*apg4::LEU2* Δ*apg12::HIS3*	this study

the complex plays a role in vesicular sorting, allowing those containing Aut7p–PE and/or the Apg12p–Apg5p conjugate to be delivered to the pre-autophagosomal structure. There is also a third possibility, that the PI3-kinase complex provides the pre-autophagosomal structure with phosphatidylinositol 3-phosphate (PI3P); PI3P then mediates the localization of the Apg12p–Apg5p conjugate and Aut7p–PE to the structure. Analysis of the autophagy-specific PI3-kinase during the organization of the pre-autophagosomal structure will further the understanding of general membrane dynamics mediated by PI3-kinases.

Here, we define a pre-autophagosomal structure, which is directly involved in the formation of autophagosomes. We also propose specific interrelationships between the many *APG* genes. This report provides insights into the precise functions of Apg proteins.

Materials and methods

Yeast strains and media

Yeast strains used in this study are listed in Table II. We used standard methods for yeast manipulation (Kaiser *et al*., 1994). Cells were grown in either YEPD (1% yeast extract, 2% peptone and 2% glucose) or SD + CA medium (0.17% yeast nitrogen base without amino acid and ammonium sulfate, 0.5% ammonium sulfate, 0.5% casamino acid and 2% glucose) supplemented with 0.002% adenine sulfate, 0.002% tryptophan and 0.002% uracil if necessary. Autophagy was induced in growth media containing either 0.5 or 1 μg/ml rapamycin (Sigma). To induce nitrogen starvation, the cells were incubated in SD (–N) medium (0.17% yeast nitrogen base without amino acid or ammonium sulfate, with 2% glucose). Yeast extract, yeast nitrogen base without amino acid and

ammonium sulfate, and casamino acid were obtained from Difco. Peptone, glucose, ammonium sulfate, adenine sulfate, tryptophan and uracil were purchased from Wako Pure Chemical Industries, Ltd.

Plasmids

In this study, centromeric plasmids were used to produce physiological levels of expression. The pRS316 GFP–AUT7 plasmid was created by substituting the 3× haemagglutinin sequence immediately after the start codon of the AUT7 open reading frame (ORF) in pTK108 (Kirisako *et al*., 1999) with a modified GFP sequence (S65T), following digestion by *Bam*HI. The pRS316 GFP–AUT7FG plasmid was created by substituting the 3× myc sequence immediately after the start codon of the pRS316 AUT7FG (Kirisako *et al*., 2000). The pRS314 ECFP–AUT7 plasmid was created by cloning an enhanced CFP (ECFP) fragment, amplified from pECFP (Clontech), into pRS316 GFP–AUT7 digested with *Bam*HI. From the resulting pRS316 ECFP–AUT7, we subcloned an excised *Sac*I–*Xho*I fragment into pRS314. The pRS314 APG5–GFP and the pRS416 APG9–GFP plasmids were the generous gifts of Dr D.J.Klionsky (University of Michigan). Site-directed mutagenesis using QuikChange (Stratagene) was used to insert a *Bam*HI site into pYAPG507, immediately before the stop codon of the *APG5* ORF (Kametaka *et al*., 1998) to create the pRS316 APG5-EYFP plasmid. An enhanced YFP (EYFP) fragment was amplified from pEYFP (Clontech), digested with *Bam*HI and cloned into the *Bam*HI site of pYAPG507.

The pRS316 YFP–APG1 plasmid was created by inserting the *Bam*HI cassette of EYFP immediately after the start codon of the *APG1* ORF. Site-directed mutagenesis then inserted a *Bgl*II site using QuikChange The pRS314 APG16–YFP plasmid was created by inserting the *Not*I cassette of EYFP immediately before the stop codon of the *APG16* ORF (Mizushima *et al*., 1999).

Immunoblot analysis

To detect either the GFP–Aut7p or Apg12p–Apg5p–GFP conjugate, lysates were prepared from cells grown in SD + CA medium to a density of ~OD_{600} = 1 by NaOH/2-mercaptoethanol extraction with a slight modification (Horvath and Reizman, 1994). Briefly, anti-Aut7p antiserum (Kirisako *et al*., 2000) and anti-Apg12 antiserum (A.Kuma, N.Mizushima, N.Ishihara and Y.Ohsumi, in preparation), respectively, were used as the primary antibodies. To detect Apg1p and API, we utilized anti-Apg1p antiserum (Matsuura *et al*., 1997) and anti-aminopeptidase I antiserum (gift from Dr D.J.Klionsky) as the primary antibodies, respectively. Aut7p–PE was detected following SDS–PAGE in the presence of 6 M urea, as described (Kirisako *et al*., 2000). We collected cells that had been either grown in YEPD medium to a density of ~OD_{600} = 1 or then starved in SD (–N) medium. Harvested cells were then washed with distilled water and disrupted with glass beads (Sigma) for 5 min in a buffer containing 50 mM Tris–HCl pH 7.5, 150 mM NaCl, 5 mM EDTA, 5 mM EGTA, 1 mM phenylmethanesulfonyl fluoride (PMSF; Sigma) and a protease inhibitor cocktail (Complete; Roche). Cell lysates were boiled in SDS sample buffer for 5 min. Equal protein amounts (20 μg protein) were subjected to electrophoresis, transferred to PVDF membrane (Millipore) and detected with a combination of anti-Aut7p antibody and peroxidase-conjugated goat anti-rabbit IgG antibody (Seikagaku Kogyo) by the ECL system (Amersham Pharmacia Biotech). Protein concentration was measured using a BCA reagent kit (Pierce).

Microscopy

Fluorescence microscopy was performed using a DeltaVision microscope (Applied Precision). FM4-64 (Molecular Probes) was used to identify the vacuolar membrane under a fluorescence microscope. Growing cells were incubated with 1 μg/ml FM4-64 for 15 min and then chased for 30 min at 30°C. The labelled cells were visualized by fluorescence microscopy using a Texas Red filter. To observe GFP-tagged proteins under a fluorescence microscope, we employed a FITC filter. A dual band filter set for CFP and YFP (86002; Chroma Technology Corp.), was used to detect the localization of CFP- and YFP-tagged proteins. Culture temperatures were controlled with a ΔTC3 culture dish system (Bioptechs) during time-lapse video microscopy.

Immunofluorescence microscopy was performed as previously described (Nishikawa *et al*., 1994). Cells harboring the APG9–GFP plasmids were grown in SD + CA medium to a density of ~OD_{600} = 1.5. Cultures were then treated with 0.5 μg/ml rapamycin for 2 h and subsequently fixed in 5% formaldehyde. Cells were then converted into spheroplasts and permeabilized with PBS containing 0.5% Triton X-100 for 10 min at room temperature. Next, the cells were dropped onto multiwell slide glasses (Cel-line Associates), pre-coated with polylysine (Sigma). Affinity-purified anti-Aut7p antibody was used as the primary antibody, followed by incubation with the Cy5-conjugated secondary antibody (Amersham). For double labelling with GFP-tagged proteins, we used Cy5, a fluorescent dye (Ex: 649 nm and Em: 670 nm), to minimize the bleeding of the fluorescence into the GFP channel (Ex: 489 nm and Em: 511 nm). GFP and Cy5 were visualized with the FITC and the Cy5 filter sets, respectively.

ALP assay

Autophagic activities were estimated by measuring ALP activity in cells expressing a cytosolic proform of the phosphatase (Pho8Δ60p; Noda *et al*., 1995). α-naphthyl phosphate (Sigma) was used as a substrate. Pho8Δ60p is transported to the vacuole via autophagy and processed in the vacuolar lumen to become active.

Generation of the apg1ts allele

APG1 was mutagenized by previously described PCR procedures (Cadwell and Joyce, 1995). The mutagenized gene was co-transformed into YYK190 cells with a gapped pRS316 plasmid, containing portions homologous to both ends of the PCR product. Two hundred and four colonies were picked and patched onto YEPD plates, which were then incubated overnight at 30 and 37°C. Cells were then subjected to treatment with 0.4 μg/ml rapamycin at each temperature. We examined the generation of autophagic bodies under a phase-contrast microscope. Plasmids recovered from the 22 colonies that passed the initial screening were used to re-transform YYK190 cells to confirm the temperature-sensitive phenotype.

Eight strains that passed the initial screening were subjected to an ALP assay to quantify autophagic activity. YYK126 cells were transformed with each candidate plasmid. Cells were cultured in YEPD medium at 23°C; ALP activities were measured after a 6 h nitrogen starvation at 23 or 37°C. Five strains were finally confirmed as temperature-sensitive mutants. Two of the five strains exhibiting clear temperature sensitivity were used for further analysis. The plasmids recovered from these two strains possessed identical sequences. This allele was used as *apg1*^{ts}. The temperature sensitivity resulted from the following amino acid substitutions: L88H, F112L and S158P.

Acknowledgements

We would like to thank Dr Daniel J.Klionsky for kindly providing plasmids. We would also like to thank Mr Takaji Nemoto, Drs Tokuko Haraguchi and Yasushi Hiraoka for their technical advice on fluorescence microscopy. We would like to thank Dr Scott D.Emr, Ms Akiko Kuma, Mr Yoshinobu Ichimura, Drs Akio Kihara and Takahiro Shintani for their donation of cell strains, as well as their helpful discussions. We would also like to thank NIBB Center for Analytical Instruments for their technical assistance. This work was supported in part by Grants-in-Aids for Scientific Research from the Ministry of Education, Science, Sports and Culture of Japan. K.S. was supported by the Research Fellowships of the Japan Society for the Promotion of Science for Young Scientists.

References

Abeliovich,H., Darsow,T. and Emr,S.D. (1999) Cytoplasm to vacuole trafficking of aminopeptidase I requires a t-SNARE-Sec1p complex composed of Tlg2p and Vps45p. *EMBO J.*, **18**, 6005–6016.

Abeliovich,H., Dunn,W.A.,Jr, Kim,J. and Klionsky,D.J. (2000) Dissection of autophagosome biogenesis into distinct nucleation and expansion steps. *J. Cell Biol.*, **151**, 1025–1033.

Baba,M., Takeshige,K., Baba,N. and Ohsumi,Y. (1994) Ultrastructural analysis of the autophagic process in yeast: detection of autophagosomes and their characterization. *J. Cell Biol.*, **124**, 903–913.

Babst,M., Sato,T.K., Banta,L.M. and Emr,S.D. (1997) Endosomal transport function in yeast requires a novel AAA-type ATPase, Vps4p. *EMBO J.*, **16**, 1820–1831.

Cadwell,R.C. and Joyce,G.F. (1995) Mutagenic PCR. In Dieffenbach,C.W. and Dveksler,G.S. (eds), *PCR Primer*. Cold Spring Harbor Laboratory Press, Cold Spring Harbor, NY, pp. 583–589.

Darsow,T., Rieder,S.E. and Emr,S.D. (1997) A multispecificity syntaxin homologue, Vam3p, essential for autophagic and biosynthetic protein transport to the vacuole. *J. Cell Biol.*, **138**, 517–529.

Fengsrud,M., Roos,N., Berg,T., Liou,W., Slot,J.W. and Seglen,P.O. (1995) Ultrastructural and immunocytochemical characterization of

autophagic vacuoles in isolated hepatocytes: effects of vinblastine and asparagine on vacuole distributions. *Exp. Cell Res.*, **221**, 504–519.

Fengsrud,M., Erichsen,E.S., Berg T.O., Raiborg,C. and Seglen,P.O. (2000) Ultrastructural characterization of the delimiting membranes of isolated autophagosomes and amphisomes by freeze-fracture electron microscopy. *Eur. J. Cell Biol.*, **79**, 871–882.

Funakoshi,T., Matsuura,A., Noda,T. and Ohsumi,Y. (1997). Analyses of APG13 gene involved in autophagy in yeast, *Saccharomyces cerevisiae*. *Gene*, **192**, 207–213.

George,M.D., Baba,M., Scott,S.V., Mizushima,N., Garrison,B.S., Ohsumi,Y. and Klionsky,D.J. (2000) Apg5p functions in the sequestration step in the cytoplasm-to-vacuole targeting and macroautophagy pathways. *Mol. Biol. Cell*, **11**, 969–982.

Harding,T.M., Hefner-Gravink,A., Thumm,M. and Klionsky,D.J. (1996) Genetic and phenotypic overlap between autophagy and the cytoplasm to vacuole protein targeting pathway. *J. Biol. Chem.*, **271**, 17621–17624.

Horvath,A. and Reizman,H. (1994) Rapid protein extraction from *Saccharomyces cerevisiae*. *Yeast*, **10**, 1305–1310.

Huang,W.P., Scott,S.V., Kim,J. and Klionsky,D.J. (2000) The itinerary of a vesicle component, Aut7p/Cvt5p, terminates in the yeast vacuole via the autophagy/Cvt pathways. *J. Biol. Chem.*, **275**, 5845–5851.

Ichimura,Y. *et al*. (2000) A ubiquitin-like system mediates protein lipidation. *Nature*, **408**, 488–492.

Kabeya,Y., Mizushima,N., Ueno,T., Yamamoto,A., Kirisako,T., Noda,T., Kominami,E., Ohsumi,Y. and Yoshimori,T. (2000) LC3, a mammalian homologue of yeast Apg8p, is localized in autophagosome membranes after processing. *EMBO J.*, **19**, 5720–5728.

Kaiser,C., Michaelis,S. and Mitchell,A. (1994) *Methods in Yeast Genetics*. Cold Spring Harbor Laboratory Press, Cold Spring Harbor, NY.

Kamada,Y., Funakoshi,T., Shintani,T., Nagano,K., Ohsumi,M. and Ohsumi,Y. (2000) Tor-mediated induction of autophagy via an Apg1 protein kinase complex. *J. Cell Biol.*, **150**, 1507–1513.

Kametaka,S., Matsuura,A., Wada,Y. and Ohsumi,Y. (1996) Structural and functional analyses of APG5, a gene involved in autophagy in yeast. *Gene*, **178**, 139–143.

Kametaka,S., Okano,T., Ohsumi,M. and Ohsumi,Y. (1998) Apg14p and Apg6/Vps30p form a protein complex essential for autophagy in the yeast, *Saccharomyces cerevisiae*. *J. Biol. Chem.*, **273**, 22284–22291.

Kihara,A., Noda,T., Ishihara,N. and Ohsumi,Y. (2001a) Two distinct Vps34 PtdIns 3-kinase complexes function in autophagy and CPY sorting in *Saccharomyces cerevisiae. J. Cell Biol.*, **152**, 519–530.

Kihara,A., Kabeya,Y., Ohsumi,Y. and Yoshimori,T. (2001b) Beclin-phosphatidylinositol 3-kinase complex functions at the *trans*-Golgi network. *EMBO Rep.*, **2**, 330–335.

Kim,J., Dalton,V.M., Eggerton,K.P., Scott,S.V. and Klionsky,D.J. (1999) Apg7p/Cvt2p is required for the cytoplasm-to-vacuole targeting, macroautophagy and peroxisome degradation pathways. *Mol. Biol. Cell*, **10**, 1337–1351.

Kim,J., Huang,W.P. and Klionsky,D.J. (2001) Membrane recruitment of Aut7p in the autophagy and cytoplasm to vacuole targeting pathways requires Aut1p, Aut2p and the autophagy conjugation complex. *J. Cell Biol.*, **152**, 51–64.

Kirisako,T., Baba,M., Ishihara,N., Miyazawa,K., Ohsumi,M., Yoshimori,T., Noda,T. and Ohsumi,Y. (1999) Formation process of autophagosome is traced with Apg8/Aut7p in yeast. *J. Cell Biol.*, **147**, 435–446.

Kirisako,T. *et al*. (2000) The reversible modification regulates the membrane-binding state of Apg8/Aut7 essential for autophagy and the cytoplasm to vacuole targeting pathway. *J. Cell Biol.*, **151**, 263–276.

Klionsky,D.J. and Ohsumi,Y. (1999) Vacuolar import of proteins and organelles from the cytoplasm. *Annu. Rev. Cell. Dev. Biol.*, **15**, 1–32.

Liang,X.H., Jackson,S., Seaman,M., Brown,K., Kempkes,B., Hibshoosh,H. and Levine,B. (1999) Induction of autophagy and inhibition of tumorigenesis by *beclin 1*. *Nature*, **402**, 672–676.

Matsuura,A., Tsukada,M., Wada,Y. and Ohsumi,Y. (1997) Apg1p, a novel protein kinase required for the autophagic process in *Saccharomyces cerevisiae*. *Gene*, **192**, 245–250.

Mizushima,N., Noda,T., Yoshimori,T., Tanaka,Y., Ishii,T., George, M.D., Klionsky,D.J., Ohsumi,M. and Ohsumi,Y. (1998) A protein conjugation system essential for autophagy. *Nature*, **395**, 395–398.

Mizushima,N., Noda,T. and Ohsumi,Y. (1999) Apg16p is required for the function of the Apg12p–Apg5p conjugate in the yeast autophagy pathway. *EMBO J.*, **18**, 3888–3896.

Mizushima,N., Yamamoto,A., Hatano,M., Kobayashi,Y., Kabeya,Y., Suzuki,K., Tokuhisa,T., Ohsumi,Y. and Yoshimori,T. (2001) Dissection of autophagosome formation using Apg5-deficient mouse embryonic stem cells. *J. Cell Biol.*, **152**, 657–667.

Nishikawa,S., Hirata,A. and Nakano,A. (1994) Inhibition of endoplasmic reticulum (ER)-to-Golgi transport induces relocalization of binding protein (BiP) within the ER to form the BiP bodies. *Mol. Biol. Cell*, **5**, 1129–1143.

Noda,T. and Ohsumi,Y. (1998) Tor, a phosphatidylinositol kinase homologue, controls autophagy in yeast. *J. Biol. Chem.*, **273**, 3963–3966.

Noda,T., Matsuura,A., Wada,Y. and Ohsumi,Y. (1995) Novel system for monitoring autophagy in the yeast *Saccharomyces cerevisiae*. *Biochem. Biophys. Res. Commun.*, **210**, 126–132.

Noda,T., Kim,J., Huang,W.P., Baba,M., Tokunaga,C., Ohsumi,Y. and Klionsky,D.J. (2000) Apg9p/Cvt7p is an integral membrane protein required for transport vesicle formation in the Cvt and autophagy pathways. *J. Cell Biol.*, **148**, 465–480.

Petiot,A., Ogier-Denis,E., Blommaart,E.F., Meijer,A.J. and Codogno,P. (2000) Distinct classes of phosphatidylinositol 3′-kinases are involved in signaling pathways that control macroautophagy in HT-29 cells. *J. Biol. Chem.*, **275**, 992–998.

Raymond,C.K., Howald-Stevenson,I., Vater,C.A. and Stevens,T.H. (1992) Morphological classification of the yeast vacuolar protein sorting mutants: evidence for a prevacuolar compartment in class E *vps* mutants. *Mol. Biol. Cell*, **3**, 1389–1402.

Scott,S.V., Baba,M., Ohsumi,Y. and Klionsky,D.J. (1997) Aminopeptidase I is targeted to the vacuole by a nonclassical vesicular mechanism. *J. Cell Biol.*, **138**, 37–44.

Seglen,P.O. (1987) Regulation of autophagic protein degradation in isolated liver cells. In Glaumann,H. and Ballard,F.J. (eds), *Lysosomes: Their Role in Protein Breakdown*. Academic Press, London, pp. 371–414.

Shintani,T., Mizushima,N., Ogawa,Y., Matsuura,A., Noda,T. and Ohsumi,Y. (1999) Apg10p, a novel protein-conjugating enzyme essential for autophagy in yeast. *EMBO J.*, **18**, 5234–5241.

Shintani,T., Suzuki,K., Kamada,Y., Noda,T. and Ohsumi,Y. (2001) Apg2p functions in autophagosome formation on the perivacuolar structure. *J. Biol. Chem.*, **276**, 30452–30460.

Tanida,I., Mizushima,N., Kiyooka,M., Ohsumi,M., Ueno,T., Ohsumi,Y. and Kominami,E. (1999) Apg7p/Cvt2p: A novel protein-activating enzyme essential for autophagy. *Mol. Biol. Cell*, **10**, 1367–1379.

Tsukada,M. and Ohsumi,Y. (1993) Isolation and characterization of autophagy-defective mutants of *Saccharomyces cerevisiae*. *FEBS Lett.*, **333**, 169–174.

Vida,T.A. and Emr,S.D. (1995) A new vital stain for visualizing vacuolar membrane dynamics and endocytosis in yeast. *J. Cell Biol.*, **128**, 779–792.

Yuan,W., Strømhaug,P.E. and Dunn,W.A., Jr (1999) Glucose-induced autophagy of peroxisomes in *Pichia pastoris* requires a unique E1-like protein. *Mol. Biol. Cell*, **10**, 1353–1366.

Received May 16, 2001; revised August 14, 2001; accepted September 6, 2001